



Integration of Probability Based Ridge Variation Information with Local Ridge Orientation for Fingerprint Liveness Detection

Sania Saeed¹, Hassan Dawood¹, Rubab Mehboob¹, Hussain Dawood¹

¹ University of Engineering and Technology Taxila

* Correspondence: Sania Saeed, Email ID: saniasaeed363@gmail.com

Citation | Saeed. S, Dawood. H, Mehboob. R, Dawood. H. "Integration of Probability Based Ridge Variation Information with Local Ridge Orientation for Fingerprint Liveness Detection". International Journal of Innovations in Science and Technology, Vol 4, Issue 1, pp: 189-200, 2022.

Received | Feb 18, 2022; Revised | Feb 26, 2022 Accepted | Feb 26, 2022; Published | Feb 27, 2022.

Abstract.

Fingerprints are commonly used in biometric systems. However, the authentication of these systems became an open challenge because fingerprints can easily be fabricated. In this paper, a hybrid feature extraction approach named Integration of Probability Weighted Spatial Gradient with Ridge Orientation (IPWSGR_o) has been proposed for fingerprint liveness detection. IPWSGR_o integrates intensity variation and local ridge orientation information. Intensity variation is computed by using probability-weighted moments (PWM) and second order directional derivative filter. Moreover, the ridge orientation is estimated using rotation invariant Local Phase Quantization (LPQ^{ri}) by retaining only the significant frequency components. These two feature vectors are quantized into predefined intervals to plot a 2-D histogram. The support vector machine classifier (SVM) is then used to determine the validity of fingerprints as either live or spoof. Results are obtained by applying the proposed technique on three standard databases of LivDet competition 2011, 2013, and 2015. Experimental results indicate that the proposed method is able to reduce the average classification error rates (ACER) to 5.7, 2.1, and 5.17% on LivDet2011, 2013, and 2015, respectively.

Keywords: PWM, Ridge Orientation, Feature integration, Ridge variation, ridge-valley pattern, Higher-order derivative.

INTRODUCTION

Biometric authentication is extensively encouraged to be used in security based applications for the accurate recognition of the individual on the basis of their unique biological traits and hence reduce the vulnerabilities of traditional authentication systems e.g., user name and password or secret pin codes, etc [1]. Some of the biological characteristics of individuals are defined to be used for recognition and are sub-divided into two main classes named as physiological features (fingerprints, iris, hand, and face, etc.), and behavioral features (signatures style, and voice, etc.) [2]. However, fingerprint-based

authentication is most commonly used in various security applications, most probably due to certain distinct properties of fingerprints such as persistence, consistency, and convenience [1]. With the rapid advancement in fingerprint-based biometric systems, they are more exposed to spoof attacks and can easily be fabricated via spoof materials like gelatin, silicon, wood glue, and paraffin, etc. [2]. In order to combat spoofing attacks and to enhance the security of user's personal information, fingerprint liveness detection (FLD) is the widely used approach to recognize either a sampled image is live or spoof. On the basis of characteristics, fingerprint features are categorized into Level 1 (ridge pattern), Level 2 (minutiae) and Level 3 (sweat pores, edge contours) feature [2]. In recent years, several hardware and software-based techniques have been proposed to solve FLD problems [3].

Hardware-based approaches require additional components that examine certain life signs in fingerprints such as temperature, odor, pulse, conductivity, or blood pressure [1] [2]. However, the improper assimilation of sensors can reduce the accuracy of the system. Therefore, to get higher performance and competitive solutions for liveness detection, software-based approaches are considered as its alternative and gain more interest in recognition systems [1]. Alternatively, in software-based approaches different local and global feature descriptors have been proposed to solve the FLD problem. An initial study by Abhyankar and Schuckers [4] in fingerprint liveness detection was to extract high-dimensional features from the inherent multi-resolution texture and local ridge frequencies. Liu and Cao [5] proposed a minutiae extraction algorithm from Level 1 features using the frequency modulation (FM) model. Despite the fact that Level 3 features are difficult to extract, Johnson and Schuckers [6] suggested that observing perspiration phenomena and pore location helps in liveness detection. Labati et al. [7] proposed a CNN-based technique for extraction and estimation of pore coordinates. However, a pore-based feature extraction scheme requires high-resolution fingerprint images. Local Binary Pattern (LBP) [8], Local Phase Quantization (LPQ) [9], Weber Local Descriptor (WLD) [10], Local Contrast Phase Descriptor (LCPD) [11], and Binary Statistical Image Feature (BSIF) [12], etc., are commonly used descriptors for extracting significant textural information. Local Binary Pattern (LBP) [8] is a rotational-invariant descriptor that extracts textural features from the grey-level image. However, its performance degrades in case of intensity variations and it also contains limited information. Therefore, different variants of LBP including LCP (Local coherence pattern) [13], LTP (Local ternary pattern) [14], LDP (Local derivative pattern) [15], and LTriDP (Local tri-directional patterns) [14] had been proposed in the literature to enhance the effectiveness of the LBP.

Weber Local Descriptor (WLD) proposed by Chen et al. [10] extracts only horizontal and vertical information of central pixel and only extracts limited information. Later on, Xia et al. proposed [1] an improved descriptor named Weber Local Binary Descriptor (WLBD) that mainly overcomes the main limitations related to the orientation and calculation model of the original WLD. Gragnaniello et al. [16] combines the contrast and phase information using Local Contrast and Phase Descriptor (LCPD). Combined Shepard Magnitude and Orientation (SMOc) [17] descriptor combines gradient and orientation information. Quantized Fundamental Fingerprint Features (Q-FFF) [18] integrates Level 1 and Level 3 features effectively.

Deep learning approaches are also used for the extraction of deep and robust features. Sajjad et al. [19] proposed a two-tier approach and used Convolution Neural

Network (CNN) for FLD problems. Uliyan et al. [20] used layered architecture models for deep learning of detailed features for the recognition of forged fingerprints. Jian et al. [21] employed a Densely Connected Convolutional Network and applied a genetic algorithm approach to optimize its structure.

As in FLD, edges contain most of the information and accuracy may be degraded due to the elimination of textural or sharp edge details. In existing approaches, different smoothing operators such as averaging operators or Gaussian smoothing [17] is used that over smoothens the image and suppresses the strong edge information for liveness detection. Therefore, for better edge preservation probability-weighted moments PWM was successfully used in image deblurring [22], dehazing [23] but never used for fingerprint liveness detection.

The literature study shows that there is a need for a descriptor that extracts significant ridge information by minimizing the ACER. In this paper, a feature descriptor named Integration of Probability Weighted Spatial Gradient and Ridge Orientation (IPWSGR_o) has been proposed that integrates the ridge variation and significant ridge orientations for liveness detection.

The rest of paper is organized as follows. Section 2 describes the methodology of proposed work (IPWSGR_o). Experimental analysis is discussed in Section 3 and finally Section 4 concludes the work.

Proposed Methodology

(IPWSGR_o) descriptor extracts information by observing fingerprint image both in spatial and frequency domain. Figure 1. Shows the feature extraction mechanism of the proposed descriptor.

And its main steps are discussed in this section.

1. Ridge variations along vertical and horizontal direction are obtained by the probability estimation and second order directional derivatives.
2. Ro is computed for fingerprint ridge orientation.
3. Feature set is then obtained by the integration of these two information sets i.e. spatial intensity information and local ridge (R_o) information.

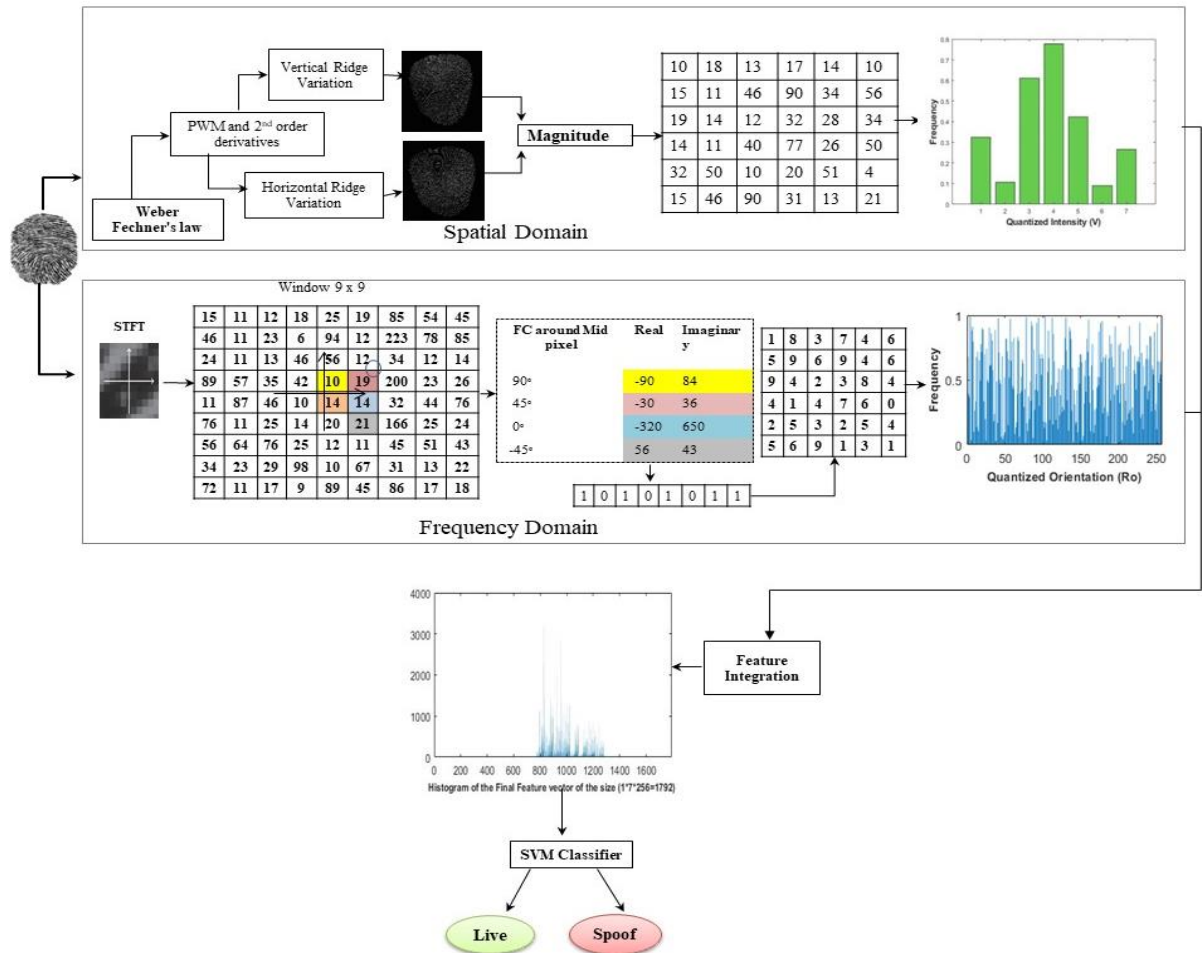


Figure 1. Proposed Descriptor for the extraction of ridge variation and orientation in Fingerprint.

Extraction of Fingerprints Ridge Variation information

In the proposed methodology, we combined probability-based ridge information and 2nd order directional derivatives for the computation of local intensity variation in the horizontal and vertical direction. Initially, an input image is taken and preprocessed by applying Fechner's law [24]. The logarithmic function in Fechner's law suppresses the abrupt behavior in pixel intensities. This law is mathematically represented as.

$$P_i = r * \log(I_i) \quad (1)$$

Considering the perceived intensity of pixel P_i as a 2-D vector, horizontal and vertical gradients are computed to extract the better ridge information. In IPWSGR, two different gradients along x-y direction are computed. Equation (2)-(3) computes the gradient by using the probability weighted moments as it extracts better ridges even in the presence of outliers and Equation (4)-(5) calculates the 2nd order gradient.

$$\nabla g_x = PWM_x(P_i) \quad (2)$$

$$\nabla g_y = PWM_y(P_i) \quad (3)$$

$$\nabla^2 g_x = D_{xx}(x, y, \sigma) \quad (4)$$

$$\nabla^2 g_y = D_{yy}(x, y, \sigma) \quad (5)$$

Equation (6)-(7) computes the variations using Shepherd similarity along horizontal and vertical directions, respectively.

Applying exponential transform lowers the intra region variations and resultantly fine edge detail is obtained. The magnitude of net variation along x-y directions is then computed using Equation (8).

$$\mathcal{L}^x = \nabla g_x \cdot e^{-|\nabla^2 g_x|} \quad (6)$$

$$\mathcal{L}^y = \nabla g_y \cdot e^{-|\nabla^2 g_y|} \quad (7)$$

$$\mathcal{L} = \sqrt{\mathcal{L}^x^2 + \mathcal{L}^y^2} \quad (8)$$

Ridge orientation Information Ro

As fingerprint contains non-periodic ridge-valley patterns therefore we need to analyze the entire image in the frequency domain. For local orientation estimation of pixels in K_n neighborhoods, we use a rotational invariant version of Local Phase Quantization (LPQⁿ). As LPQⁿ extracts information by dividing the observed image I into 'n' number of patches $P_n \in \{p_1, p_2, p_3, \dots, p_n\}$, each of the size 9x9. For each patch P_n , STFT ($I_x(u)$) is computed for each pixel of M points uniformly placed on the circle of radius r . The real and imaginary components computed at these frequencies are given by $v_i = r(\sin \phi_i, \cos \phi_i)$ where $\phi_i = 2\pi i/M$ and $i = 0, 1, 2, \dots, (M-1)$. Mathematically formulated as follows:

$$I_x(u) = \sum_y I(y) w(y - x) e^{-j2\pi u y} \quad (9)$$

For local ridge orientation estimation real and imaginary values of only four frequencies oriented at angle 0°, 45°, -45° and 90° degree are considered. Then real and imaginary values for each of selected frequencies are computed by means of STFT and binary quantized to form 8-bit feature vector $\hat{q} = \{q_1, q_2, \dots, q_8\}$ represented as an integer value ranging from 0-255 using the following equation.

$$\hat{q} = \sum_{i=1}^8 q_i 2^{i-1} \quad (10)$$

Resultantly, we obtain a feature vector $[F_x(v_0), \dots, F_x(v_{M-1})]$. The sign of real and imaginary component contains some phase information. From this vector we just retain the sign associated with the imaginary part as $S_i = \{s_0, s_1, \dots, s_{m-1}\}$. Characteristic

ridge orientation (R_0) is then calculated using the Equation (11). Similarly characteristic orientation of the rotated patch at angle θ is given by $R_0(x) + \theta$

$$R_0(x) = \sum_{i=0}^{M-1} s_i e^{j\varphi_i} \quad (11)$$

Integration of ridge variation and orientation features

The final feature vector is obtained by the integration of the ridge variation features and local ridge orientation (R_0) features computed in spatial and frequency domain respectively. These two feature sets are then quantized for the dimensionality reduction and robust recognition. Intensity Variation feature are quantized into V quantization intervals while frequency domain features are binned into M levels. Resultantly the dimension of final feature vector is $1 \times VM$. Experimental analysis shows that better results are obtained by taking the value of $V = 7$ and $M = 256$. The final quantized feature vector obtained over the entire image is represented in the form of 2-D histogram.

RESULTS AND DISCUSSION

This section at first provides the description of databases used for experimentation and the optimal parameter selection is described for the evaluation of IPWSGR_o. After that, the results of the proposed descriptor along with the chosen parameter are recorded and show the accuracies and error rates on each dataset.

Dataset

Three standard databases of LivDet competition i.e. LivDet 2011 [25], LivDet 2013 [26] and LivDet 2015 [27] are used to assess the performance of our proposed descriptor. Different sensors named Biometrika, Digital Persona, Italdat, Swipe, Greenbit, Hi-scan, and Sagem are used to capture the fingerprint images. Most of the fake samples in these databases are generated by fabricating the live samples using different spoofing material along with the support of users that better helps in making the fake samples. All datasets contain their independent training and testing sets. Each set has 2000 images belongs to two different classes i.e. live and spoof. Training set images are used to train the proposed model while performance evaluation of the model is done on the test set.

Evaluation matrices for Live and Fake error rates

The performance of IPWSGR_o is evaluated by measuring the accuracy of the proposed descriptor and average classification error rate (ACER). Both these parameters i.e. accuracy and ACER are mathematically represented in Equation 12 and Equation 13) respectively. Let we denote total number of testing images by N_t and correctly classified live and fake images as N_i .

$$Acc = \left(\frac{1}{N_t} \sum_{c=1}^{N_t} N_j \right) \times 100 \quad (12)$$

ACER is computed by taking average of live and fake error rates as follows:

$$ACER = \frac{LER + FER}{2} \quad (13)$$

The term live error rate (LER) represents the misclassified live fingerprint images and incorrectly taken as fake ones mathematically represented as:

$$LER = \frac{\text{misclassified live image}}{\text{total number of live images}} \times 100 \quad (14)$$

Similarly, fake error rate represents the misclassification of spoof fingerprint images and incorrectly taken as real or live images mathematically represented as:

$$FER = \frac{\text{misclassified spoof image}}{\text{total number of spoof images}} \times 100 \quad (12)$$

Average classification error rates, live and spoof error rates, and accuracy on LivDet 2011, 2013, and 2015 are observed individually and recorded in **Table 1**. However, optimized results are obtained by setting the appropriate value of RBF-sigma. It is evident from the results reported in **Table 1**, that the spoof error rate is considerably higher as compared to the live error rates in some of the cases. For instance, the significantly higher spoof error rate of 14.2% is obtained on Italdeta (LivDet 2011). Similarly, considerable higher fake error rates of 3.3, 2.1, and 4.1% are obtained on all the datasets of LivDet 2013. Likewise, higher spoof error rates of 2.25 and 7.5% are obtained on Greenbit and Hi-Scan (LivDet 2013). Like silicone, gelatin makes the perfect copy of a fingerprint, similar to that of a real one hence are more difficult to recognize. To evaluate the impact of spoof material on error rates, experiments on Biometrika and Italdeta (LivDet 2013) have been performed and results are presented in Table 2. Five different spoofing materials are used for fabricating fingerprints of Biometrika and Italdeta (2013) such as EcoFlex, gelatin, WoodGlue, latex and Modasil. Obtained results depict that the error rate while using "latex" material is high for both Biometrika and Italdeta and it may affect the overall accuracy.

Table 1. Average classification error rate, live error rate, and spoof error rate on Livedet2011, Livedet2013, and Livedet2015.

Dataset		err_{live}	err_{spoof}	AER	Accuracy (%)
LivDet 2011	Biometrika	3.7	4.6	4.15	95.85
	Digital Persona	4.7	5.3	5.00	95.00
	Italdeta	6.5	14.2	10.3	89.65
	Sagem	3.8	3.1	3.48	96.52
LivDet 2013	Biometrika	0.8	3.3	2.05	97.95
	Italdeta	0.2	2.1	1.15	98.85
	Swipe	2.1	4.1	3.10	96.9
	Crossmatch	5.33	4.83	5.08	94.92
LivDet 2015	Digital Persona	9.3	6.9	8.10	91.9
	Greenbit	2.0	2.24	2.12	97.88
	Hi-Scan	3.3	7.5	5.4	94.6

Table 2. Live and fake error rates on different spoofing material of Biometrika and Italdeta of LivDet2013

Train Set	Test Set	Biometrika	Italdeta
Feb 2022	Vol 4 Issue 1		Page 195

Live+ EcoFlex	Live+ EcoFlex	0.33	0.08
Live+Gelatin	Live+Gelatin	0.83	1.75
Live+Latex	Live+Latex	3.5	2.0
Live+Modasil	Live+Modasil	2.33	0.83
Live+Woodglue	Live+Woodglue	2.75	1.00

Performance comparison of IPWSGR_o with state-of-the-art methods

In the proposed method IPWSGR_o outperforms state-of-the-art methods. Table 3, Table 4 and Table 5 shows the performance comparison of LivDet2011, 2013 and 2015 with state-of-the-art techniques respectively.

Table 3. Performance comparison of the proposed descriptor on Livedet2011, with state-of-the-art Techniques.

Methods	Biometrika	Digital Persona	Italdata	Sagem	ACER
WLD [10]	13.3	13,8	27.7	6.7	15.37
SMOc [17]	4.9	5.0	11.1	2.5	5.87
WLBD [1]	5.65	4.1	11.85	2.25	5.96
LCPD [11]	4.9	4.7	12.3	3.2	6.28
DCNNISE[28]	9.2	1.35	12.35	2.9	6.45
CNN [29]	9.9	1.9	5.1	7.9	6.2
DenseNet[21]	7.70	5.95	12.25	5.12	7.76
Proposed method	4.15	5.0	10.35	3.48	5.75

Table 4. Performance comparison of the proposed descriptor on Livedet2013 with other state-of-the-art techniques.

Methods	Biometrika	Italdata	Swipe	ACER
WLD [10]	5.2	7.1	8.4	6.90
SMOc [17]	1.6	1.4	3.8	2.2
LCPD [11]	1.2	1.3	4.7	2.4
BSIF [12]	1.1	3.0	5.2	3.1
CNN [29]	4.6	47.7	6.0	19.4
DCNNISE [28]	4.35	1.4	2.05	2.6
DenseNet [21]	2.70	2.00	10.74	5.1
FLDNet [21]	2.60	2.15	7.26	4.00
Proposed Method	2.05	1.15	3.10	2.1

Table5. Performance comparison of the proposed descriptor on Livdet2015 with other state-of-the-art methods.

Methods	Crossmatch	Digital Persona	Greenbit	Hi-Scan	ACER
SMOc [17]	6.40	8.70	2.93	3.15	5.3

WLBD [1]	10.82	13.72	4.35	9.64	9.67
WLD [30]	12.39	15.24	8.69	20.7	14.27
ROI [31]	3.46	6.8	4.77	6.24	5.32
ROI+LGP [31]	5.16	8.8	4.93	5.56	6.11
Proposed Method	5.08	8.10	2.12	5.4	5.17

In Table 3 proposed descriptor obtains better accuracy and least error rate of the value 4.15% on Biometrika of LivDet 2011. Results reported in Table 4 shows that the error rate on the Italdeta images is minimized up to 1.15%. This might be because of the usage of lower quality spoof samples in Italdeta of LivDet 2013. As latent fingerprints are used in the spoof creation process, therefore these fingerprints are easily recognizable. It has been observed in Table 5, that IPWSGR_o increased the accuracy on Crossmatch, Digital Persona, and Green-bit as compared to state-of-the-art methods. The classification performance of the proposed descriptor degrades on the Hi-Scan images due to the presence of high-resolution images. It is worth noticing from Table 3 that IPWSGR_o outperformed in many state-of-the-art handcrafted feature extraction methods as well as from deep learning approaches.

While using IPWSGR_o, the ACER reduces to 0.53% from LCPD [11], 0.12% from SMOc [17], 9.62% from WLD [10], 0.21% from WLBD [1], 0.7% from DCNNISE [28] in the comparison table of LivDet2011. From T, we observe that ACER reduces to 0.3% from LCPD [11], 0.1% from SMOc [17], 4.8% from WLD [10], 0.5% from DCNNISE [28], and 1% from BSIF [12]. Similarly, in Table 5 the proposed descriptor outperformed as compared to state-of-the-art methods such as from SMOc [17] by 0.13%, WLD [30] by 9.1%, and from WLBD [1] by 4.5%. LBP is commonly used to extract small textural details and its performance degrades in case of intensity variation. In BSIF [12], random samples are selected that resultantly missed the potential information and hence degrades the detection accuracy. Significant ridge information may be lost in WLD [10] due to the consideration of only horizontal and vertical direction pixels by its orientation component. In current FLD techniques including SMOc [17], LCPD [11] and WLBD [1] incorporate both local and global features and have achieved the best results with minimal ACER but these methods. In SMOc [17], due to the use of a simple gradient function only limited information have been extracted resultantly leads to the loss of significant intensity variation information. In the proposed method IPWSGR_o outperforms these methods.

The ridge extraction component of IPWSGR_o uses 2nd order gradients and PWM that incorporates the significant ridge variations that may be neglected in the previous techniques. Additionally, R_o component of proposed descriptor extracts significant ridge orientation information by using LPQ^{ri} and excluding the irrelevant details. Hence, due to the fusion of these two significant information sets, computational complexity can be reduced, and better minimal error rates are obtained. Techniques that have low ACER are represented in bold. Experimental analysis shows that our framework obtains lower average error rates than the existing methods.

CONCLUSION

This paper aims to presents a robust feature descriptor for FLD. Proposed descriptor uses PWM and higher-order gradient operator for extracting potential ridge variation information in the spatial domain and extracts the significant ridge orientation information using a rotational invariant LPQⁿ. Both feature sets are then quantized into predefined intervals for dimensionality reduction. Experimental results on the LivDet 2011, 2013, and 2015 datasets indicate that our proposed descriptor achieves higher accuracy with minimal ACER than state-of-the-art descriptors. Therefore, our future work aims to lessen the noise without losing the important information. Moreover, in the future deep learning approaches and level 2 features (i.e., minutiae points) will also be incorporated to obtain a more significant feature set.

Acknowledgment. Acknowledgments are considered necessary.

Author's Contribution. All the authors contributed equally in this work.

Conflict of interest. Authors claim that there exists no conflict of interest for publishing this manuscript in IJIST.

REFERENCES

- [1] Z. Xia, C. Yuan, R. Lv, X. Sun, N. N. Xiong, and Y. Q. Shi, "A novel weber local binary descriptor for fingerprint liveness detection," *IEEE Trans. Syst. Man, Cybern. Syst.*, vol. 50, no. 4, 2020, doi: 10.1109/TSMC.2018.2874281.
- [2] Z. Xia, C. Yuan, X. Sun, D. Sun, and R. Lv, "Combining wavelet transform and LBP related features for fingerprint liveness detection," *IAENG Int. J. Comput. Sci.*, vol. 43, pp. 290–298, 2016.
- [3] Z. Xia, R. Lv, Y. Zhu, P. Ji, H. Sun, and Y. Q. Shi, "Fingerprint liveness detection using gradient-based texture features," *Signal, Image Video Process.*, vol. 11, no. 2, 2017, doi: 10.1007/s11760-016-0936-z.
- [4] A. Abhyankar and S. Schuckers, "Fingerprint liveness detection using local ridge frequencies and multiresolution texture analysis techniques," 2006, doi: 10.1109/ICIP.2006.313158.
- [5] E. Liu and K. Cao, "Minutiae Extraction from Level 1 Features of Fingerprint," *IEEE Trans. Inf. Forensics Secur.*, vol. 11, no. 9, 2016, doi: 10.1109/TIFS.2016.2541345.
- [6] P. Johnson and S. Schuckers, "Fingerprint pore characteristics for liveness detection," in *Lecture Notes in Informatics (LNI), Proceedings - Series of the Gesellschaft fur Informatik (GI)*, 2014, vol. P-230.
- [7] R. Donida Labati, A. Genovese, E. Muñoz, V. Piuri, and F. Scotti, "A novel pore extraction method for heterogeneous fingerprint images using Convolutional Neural Networks," *Pattern Recognit. Lett.*, vol. 113, 2018, doi: 10.1016/j.patrec.2017.04.001.
- [8] T. Ojala, M. Pietikäinen, and T. Mäenpää, "Multiresolution gray-scale and rotation invariant texture classification with local binary patterns," *IEEE Trans. Pattern Anal. Mach. Intell.*, vol. 24, no. 7, 2002, doi: 10.1109/TPAMI.2002.1017623.
- [9] L. Ghiani, G. L. Marcialis, and F. Roli, "Fingerprint liveness detection by local phase quantization," 2012.
- [10] J. Chen *et al.*, "WLD: A robust local image descriptor," *IEEE Trans. Pattern Anal. Mach. Intell.*, vol. 32, no. 9, 2010, doi: 10.1109/TPAMI.2009.155.
- [11] D. Gragnaniello, G. Poggi, C. Sansone, and L. Verdoliva, "An Investigation of Local Descriptors for Biometric Spoofing Detection," *IEEE Trans. Inf. Forensics Secur.*, vol. 10,

- no. 4, 2015, doi: 10.1109/TIFS.2015.2404294.
- [12] L. Ghiani, A. Hadid, G. L. Marcialis, and F. Roli, "Fingerprint Liveness Detection using Binarized Statistical Image Features," 2013, doi: 10.1109/BTAS.2013.6712708.
- [13] W. Kim, "Fingerprint Liveness Detection Using Local Coherence Patterns," *IEEE Signal Process. Lett.*, vol. 24, no. 1, 2017, doi: 10.1109/LSP.2016.2636158.
- [14] M. Verma and B. Raman, "Local tri-directional patterns: A new texture feature descriptor for image retrieval," *Digit. Signal Process. A Rev. J.*, vol. 51, 2016, doi: 10.1016/j.dsp.2016.02.002.
- [15] B. Zhang, Y. Gao, S. Zhao, and J. Liu, "Local derivative pattern versus local binary pattern: Face recognition with high-order local pattern descriptor," *IEEE Trans. Image Process.*, vol. 19, no. 2, 2010, doi: 10.1109/TIP.2009.2035882.
- [16] D. Gragnaniello, G. Poggi, C. Sansone, and L. Verdoliva, "Local contrast phase descriptor for fingerprint liveness detection," *Pattern Recognit.*, vol. 48, no. 4, 2015, doi: 10.1016/j.patcog.2014.05.021.
- [17] R. Mehboob, H. Dawood, H. Dawood, M. U. Ilyas, P. Guo, and A. Banjar, "Live fingerprint detection using magnitude of perceived spatial stimuli and local phase information," *J. Electron. Imaging*, vol. 27, no. 05, 2018, doi: 10.1117/1.jei.27.5.053038.
- [18] A. Alshdadi, R. Mehboob, H. Dawood, M. O. Alassafi, R. Alghamdi, and H. Dawood, "Exploiting Level 1 and Level 3 features of fingerprints for liveness detection," *Biomed. Signal Process. Control*, vol. 61, 2020, doi: 10.1016/j.bspc.2020.102039.
- [19] M. Sajjad *et al.*, "CNN-based anti-spoofing two-tier multi-factor authentication system," *Pattern Recognit. Lett.*, vol. 126, 2019, doi: 10.1016/j.patrec.2018.02.015.
- [20] D. M. Uliyan, S. Sadeghi, and H. A. Jalab, "Anti-spoofing method for fingerprint recognition using patch based deep learning machine," *Eng. Sci. Technol. an Int. J.*, vol. 23, no. 2, 2020, doi: 10.1016/j.jestch.2019.06.005.
- [21] W. Jian, Y. Zhou, and H. Liu, "Densely Connected Convolutional Network Optimized by Genetic Algorithm for Fingerprint Liveness Detection," *IEEE Access*, vol. 9, 2021, doi: 10.1109/ACCESS.2020.3047723.
- [22] H. Dawood *et al.*, "Probability weighted moments regularization based blind image De-blurring," *Multimed. Tools Appl.*, vol. 79, no. 7–8, 2020, doi: 10.1007/s11042-019-7520-9.
- [23] R. M. Yousaf, H. A. Habib, Z. Mehmood, A. Banjar, R. Alharbey, and O. Aboulola, "Single image dehazing and edge preservation based on the dark channel probability-weighted moments," *Math. Probl. Eng.*, vol. 2019, 2019, doi: 10.1155/2019/9721503.
- [24] J. J. Mathew and A. P. James, "Spatial stimuli gradient sketch model," *IEEE Signal Process. Lett.*, vol. 22, no. 9, 2015, doi: 10.1109/LSP.2015.2404827.
- [25] D. Yambay, L. Ghiani, P. Denti, G. L. Marcialis, F. Roli, and S. Schuckers, "LivDet 2011 - Fingerprint liveness detection competition 2011," 2012, doi: 10.1109/ICB.2012.6199810.
- [26] L. Ghiani *et al.*, "LivDet 2013 fingerprint liveness detection competition 2013," 2013, doi: 10.1109/ICB.2013.6613027.
- [27] L. Ghiani, D. A. Yambay, V. Mura, G. L. Marcialis, F. Roli, and S. A. Schuckers, "Review of the Fingerprint Liveness Detection (LivDet) competition series: 2009 to 2015," *Image Vis. Comput.*, vol. 58, 2017, doi: 10.1016/j.imavis.2016.07.002.
- [28] C. Yuan, Z. Xia, L. Jiang, Y. Cao, Q. M. J. Wu, and X. Sun, "Fingerprint Liveness Detection Using an Improved CNN With Image Scale Equalization," *IEEE Access*, vol.

- 7, 2019, doi: 10.1109/ACCESS.2019.2901235.
- [29] S. Kim, B. Park, B. S. Song, and S. Yang, "Deep belief network based statistical feature learning for fingerprint liveness detection," *Pattern Recognit. Lett.*, vol. 77, 2016, doi: 10.1016/j.patrec.2016.03.015.
- [30] D. Gragnaniello, G. Poggi, C. Sansone, and L. Verdoliva, "Fingerprint liveness detection based on Weber Local image Descriptor," 2013, doi: 10.1109/BIOMS.2013.6656148.
- [31] C. Yuan, Z. Xia, X. Sun, and Q. M. J. Wu, "Deep Residual Network with Adaptive Learning Framework for Fingerprint Liveness Detection," *IEEE Trans. Cogn. Dev. Syst.*, vol. 12, no. 3, 2020, doi: 10.1109/TCDS.2019.2920364.



Copyright © by authors and 50Sea. This work is licensed under Creative Commons Attribution 4.0 International License.